ELSEVIER Applied Mathematics and Computation 140 (2003) 255–277

APPLIED MATHEMATICS AND COMPUTATION

www.elsevier.com/locate/amc

A transfer function technique to describe odor causing VOCs transport in a ventilated airspace with mixing/adsorption heterogeneity

Chung-Min Liao [a,*], Huang-Min Liang [a], Jein-Wen Chen [a], Jui-Sheng Chen [b]

[a] *Department of Bioenvironmental Systems Engineering, National Taiwan University, Taipei 10617, Taiwan, ROC*

[b] *Department of Environmental Engineering and Sanitation, Foo-Yin University of Technology, Kaohsiung 831, Taiwan, ROC*

Abstract

A model describing odor causing volatile organic compounds (VOC-odor) transport in a ventilated airspace influenced by heterogeneity of adsorption surface of ambient aerosol and air mixing pattern is proposed and analyzed based on a transfer function modeling technique. In this study an advection–reaction impulse/step response function for VOC-odor is assumed. The system process presented by an ensemble transfer function is solved analytically in the Laplace domain. The analytical results are then numerically inverted using a modified fast Fourier transform algorithm. The model requires the specification of probability density function for residence time of airflow and for both equilibrium linear partitioning and first-order mass transfer rate parameters to quantify the specific air mixing pattern and transport processes. The model predicts the ensemble mean VOC-odor concentrations for a variety of adsorption kinetics and mixing pattern combinations as a function of the boundary impulse/step response inputs as well as residence time and adsorption rate statistics. The general behavior of output VOC-odor profiles is analyzed through the effects of mean adsorption rate coefficient, mean linear partitioning constant, mixing efficiency, mean residence time and coefficient of variations of both linear partitioning and rate coefficients. It

* Corresponding author.
E-mail address: cmliao@ccms.ntu.edu.tw (C.-M. Liao).

PII: S0096-3003(02)00224-2

indicates that when mixing/adsorption heterogeneity exists, simple complete mixing assumption and simple distribution of rate constant is inherently not sufficient to represent a more generally distributed mixing/adsorption process of VOC-odor transport in a ventilated airspace.

Keywords: Transfer function; Mixing; Adsorption; Heterogeneity; Odor; VOCs

Nomenclature

a, b	positive constants in the linear free-energy relationships (LFERs)
$c(x,t)$	odor causing volatile organic compounds (VOC-odor) concentration, $\mathrm{kg\,m^{-3}}$
C_0	initial concentration of VOC-odor, $\mathrm{kg\,m^{-3}}$
$C^*(T,X)$	dimensionless variable of VOC-odor concentration
$\widehat{C}^*(X,s)$	Laplace-transformed $C^*(T,X)$
$\widehat{C}(X,s)$	ensemble mean of $\widehat{C}^*(X,s)$
CV_k, CV_τ	coefficients of variations of K and τ
d	constant ($d = 1 - b$)
$E[\cdot]$	mathematical expectation operator
$h(t)$	density function
$\hat{h}(s)$	transfer function for the rate-limiting processes
$\widehat{H}(s)$	ensemble mean of $\hat{h}(s)$
k	adsorption rate coefficient, $\mathrm{h^{-1}}$
k_d	linear partition coefficient between gas and solid phases at sorption equilibrium, $\mathrm{m^3\,kg^{-1}}$
K	dimensionless adsorption rate coefficient
$\overline{K}$	mean of gamma distribution of K
K_D	dimensionless equilibrium linear partitioning coefficient
$\overline{K}_\mathrm{D}$	mean linear partitioning coefficient
L_0	length of animal unit, m
P_d	gamma probability density function (pdf) of K_D
$P_{\mathrm{d}k}$	bivariate pdf of K_D and K
P_k	gamma pdf of K
P_τ	gamma pdf of τ
Q	volumetric airflow rate, $\mathrm{m^3\,s^{-1}}$
$q(x,t)$	concentration of adsorbed VOC-odor on aerosol surface, $\mathrm{kg\,m^{-3}}$
q_e	equilibrium adsorbed phase concentration, $\mathrm{kg\,kg^{-1}}$
q^*	dimensionless variable of q
$\hat{q}^*(s)$	Laplace-transformed q^*
s	Laplace variable

sd_τ, sd_k	standard deviation of gamma distributions for τ and K
t	time, h
$\bar{t}$	nominal mean residence time, h
T	dimensionless variable of t
$U(t)$	unit step function
v	air velocity, $m\,s^{-1}$
V	dimensionless variable of v
V_c	air volume occupied by complete mixing, m^3
V_i	air volume occupied by incomplete mixing, m^3
V_p	air volume occupied by piston flow, m^3
V_T	total volume in the system, m^3
x	mean direction of airflow, m
X	dimensionless variable of x

Greek letters

α_τ, β_τ	shape and scale parameters of gamma distribution of τ
α_k, β_k	shape and scale parameters of gamma distribution of K
γ	gamma distribution
ρ	aerosol density, $kg\,m^{-3}$
θ	mixing volume factor I
θ_m	surface volumetric moisture content of aerosol, v/v
τ	dimensionless residence time of VOC-odor
$\bar{\tau}$	mean of gamma distribution of τ
μ	mixing efficiency
η	mixing volume factor II
ζ	dummy variable of integration in gamma function
$\Gamma(\bullet)$	gamma function

1. Introduction

The transport of VOC-odor in a ventilated animal housing, subject to rate limitation of mass transfer between the heterogeneous mixing patterns and the interaction among VOC-odor, ambient aerosol, and adsorbed VOC-odor (or called dust-borne VOC-odor), is increasingly the focus of research in bio-environmental control engineering [1–6].

Conventional approaches to deal with the airflow mixing problem often assume that mixing patterns are homogeneous or can be represented as an equivalent complete mixing mechanism so that every mixing process can be described in a deterministic manner. It is evident that this assumption is not always valid. Barber and Ogilvie [7] suggested that departure from complete mixing might be caused by the formation of multiple flow regions within the

airspace or short-circuiting of supply air to exhaust outlet. A work presented by Chen et al. [8] regarding the methods to measure dust production and deposition rates in buildings indicated that the assumption of complete mixing was not valid during tests. Their experimental data showed that tanks-in-series flow, i.e., different flow regions behaving as a number of mixed tanks connected in series dominated the overall mixing process within the ventilated airspace. Their work also suggested that a more complicated multi-zone mixing model might be needed to account for heterogeneous mixing to better understand the behavior of dust local transport mechanisms.

Simulation models for the transport of VOC-odor in ventilated animal housing are important tools for testing our understanding of transport phenomena and for designing management strategies for creating a healthy microclimate for animals. From a management perspective, knowing both when a VOC-odor will arrive at a given location in a ventilated airspace and how much of the air exchange rate purges the VOC-odor are of extreme important.

Assessment of indoor air quality issues regarding odor/VOC-odor transport in ventilated animal housing requires the consideration of different control strategies and various air pollution control options. The decision making process leading to the optimal control strategy now relies heavily on quantitative computer models of airflow and odor transport in ventilated airspace. These approaches in turn call for model development of the pertinent physicochemical and biological processes. Thus, we need a detailed understanding of the phenomena controlling VOC-odor sorption and dust-borne VOC-odor deposition, and we must be able to rely on quantitative models, which are able to capture the main features of these processes.

For VOC-odor, a key process to include in any transport model is adsorption. Many models have assumed linear equilibrium sorption, yet many laboratory and field observations cannot be accurately simulated using the assumption of linear equilibrium sorption [4]. At the particle scale, the governing processes of kinetic adsorption/desorption are complex and poorly understood. A variety of processes, all related to the complexity and heterogeneity of VOC-odor and ambient aerosol profile occur. In addition, to particle scale processes, large scale heterogeneity can create physical nonequilibrium, due to multiple airflow regions of heterogeneous mixing and stagnant airflow, that may be observed in the transport of adsorbed and nonadsorbed VOC-odors.

A reactive VOC-odor moving through a medium of ambient aerosol or bioaerosol in the mean airflow direction x is illustrated in Fig. 1. Sorption reactions often affect the movement and fate of VOC-odor in a highly dusty livestock environment (Fig. 1A). The sorption of VOC-odor on airborne dust has been shown to be dominated by the behavior of the interactions among VOC-odor, airborne dust, and dust-borne VOC-odor [5]. The mechanistic function of airborne dust in uptake of VOC-odor may be partitioning and/or

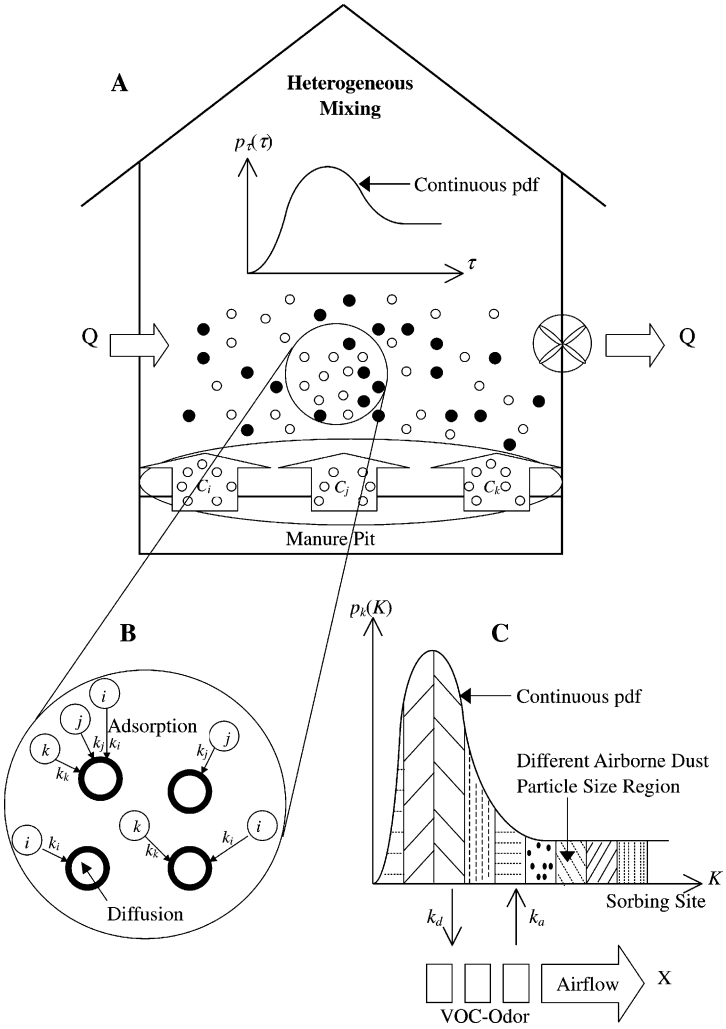

Fig. 1. An integrated scheme showing mixing/adsorption heterogeneity in a ventilated animal unit: (A) VOC-odor (◯) and airborne dust (●) mixture in a ventilated airspace where the heterogeneous air mixing is described by a continuous pdf of RTD, (B) adsorption and diffusion behaviors between VOC-odor and airborne dust where the mechanistic function of airborne dust in uptake of VOC-odor may be partitioning and/or adsorption, and (C) VOC-odor in the mean airflow direction and sorption in airborne dust medium with different particle sizes described by a continuous pdf of adsorption rate coefficient.

adsorption (Fig. 1B). The ventilated airspace is composed of a heterogeneous mixing airflow field and a continuum of sorbing surfaces of ambient aerosol/bioaerosol (Fig. 1C). The VOC-odor can be sorbed either instantaneously or

time-dependently onto a fraction of the surface of airborne dust during transport. The term "surface" here does not necessarily mean a distinct physical point but a sorbing domain or portion of the sorbing site of airborne dust envisioned as a fraction having uniform local sorption properties.

The sorption mechanisms at each surface presumed to be either a diffusion controlled process or a combination of diffusion and sorption kinetics. A nonequilibrium model has to have a sufficient capability to represent a variety of adsorption/desorption and transport mechanisms including sorption rate limitations, first-order approximations of diffusion and physical nonequilibrium. With the presence of mixing/sorption heterogeneity, nonequilibrium conditions for a given ventilated airflow system were examined.

Given the heterogeneity in air mixing, in size, shape, and composition of ambient aerosol, a stochastic approach may be incorporated and it is assumed that the residence time, sorption equilibrium constant, first-order mass transfer rate constant, and/or diffusion coefficient are continuously distributed. The objective of this paper is to generalize a dynamic transport model of VOC-odor in ventilated animal housing under heterogeneity of both air mixing and adsorption kinetics, with a pdf describing both residence time of VOC-odor, as well as adsorption rate parameters in the first-order mass transfer process approximated at a local scale.

In this paper we present a transfer function modeling technique [9] to describe the dynamic response between adsorbed- and gas-phase VOC-odor. The determination of the transfer function of a system, i.e., the determination of a dynamic input–output model that can show the effect on the output of a system subject to any given series of inputs. Transfer function model building is important because it is only when the dynamic characteristics of a system are understood that manipulation and control of the system is possible. Methods for estimating transfer function models based on deterministic perturbations of the boundary inputs such as step and impulse response functions were presented.

2. Mathematical model

2.1. Transfer function modeling

We employ here a commonly used model, a one-dimensional form of the advection–dispersion–reaction equation incorporating sorption equilibrium and rate expression [10], to describe the dynamic transport of VOC-odor in a heterogeneous mixing/sorption ventilated airspace. The transport of VOC-odor with mixing/sorption kinetics heterogeneity may be characterized by the time evolution of the VOC-odor concentration $c(x,t)$ ($\mathrm{kg\,m^{-3}}$) and the concentration of adsorbed VOC-odor (or dust-borne VOC-odor) $q(x,t)$ ($\mathrm{kg\,kg^{-1}}$)

on the ambient aerosol surface. These two concentrations are both functions of the mean airflow direction x and the time t.

Two model simplifications are inherent in our analysis: (1) neglect of local dispersion and molecular diffusion processes, and (2) neglect of ambient aerosol and adsorbed VOC-odor deposition.

Neglect of dispersion processes. This simplification represents a reasonable approximation, since only within a few airflow regions, where airborne dust concentration changes rapidly, can dispersion be important [8,11]. By excluding such regions, any dispersion effects can be safely neglected. Reliable estimates of the dispersivity that may be scale-dependent, however, are very difficult to obtain. The dispersive effect is also characterized by other limitations. Liu et al. [12] and Hoff and Bundy [13] pointed out that the theoretical foundation for the dispersive effect in multiple airflow regions is not sound for systems other than an air jet with turbulent or laminar flow. The model assumes that molecular diffusion is negligible indicating the existing gaseous or particulate contaminates and air is identical and both are related to the distribution of air velocities. This condition, however, is not that restrictive since molecular diffusion is negligible compared with mechanical dispersion in most situations, especially in large-scale systems.

Neglect of solid-phase deposition. A simple criterion to ascertain the validity of this approximation is to show that the product of the deposition rate coefficient and the average residence time is not considerably larger than unity [5]. A theoretical study by Liao et al. [5] shows that the ratios between adsorption and deposition rates for two different aerosol profiles of 2 and 8 μm geometric mean diameters in a ventilated airspace have the magnitudes ranged from about $10–10^2$. Thus, a relative comparison with adsorption and ventilation, deposition reflects an insignificant contribution to the transport mechanisms.

Although local dispersion and molecular diffusion have been omitted, the macroscopic dispersive effects retained through the ensemble approaches described later for random velocity field and its heterogeneous mixing patterns.

The equation of the single population model for the specified VOC-odor and adsorbed-phase therefore can be coupled by a simple advection–reaction equation as,

$$\frac{\partial c}{\partial t} = -v(x)\frac{\partial c}{\partial x} - \frac{\rho}{\theta_{\mathrm{m}}}\left[\frac{\partial q_{\mathrm{e}}}{\partial c}\frac{\partial c}{\partial t} - k(k_{\mathrm{d}}c - q)\right], \tag{1}$$

the second-term of right-handed side of Eq. (1) is an equilibrium adsorption isotherm, whereas the third-term is a first-order mass transfer approximation,

$$\frac{\partial q}{\partial t} = k(k_{\mathrm{d}}c - q), \tag{2}$$

where v is the air velocity ($m\,s^{-1}$), ρ is the aerosol density ($kg\,m^{-3}$), θ_m is the surface volumetric moisture content of aerosol (%, v/v), q_e is the equilibrium adsorbed phase concentration ($kg\,kg^{-1}$), k is the adsorption rate coefficient (h^{-1}), and k_d is the linear partition coefficient between gas and solid phases at sorption equilibrium ($m^3\,kg^{-1}$).

In order to simplify the complications of the aerosol geometric specification required in the diffusion formulation, we adopted the commonly used first-order mass transfer approximation (Eq. (2)) at the local scale. The rate coefficient in Eq. (2) inherently lumps all the local geometric influence as if a diffusion mechanism dominants. A first-order mass transfer or a diffusion process presented in Eq. (2) can generally use a density function describing the process of mass sorption/desorption between the mixing airspace and the sorbing surfaces. The adsorbed VOC-odor $q(x,t)$ can then be described by a convolution integral,

$$\frac{\rho}{\theta_m} q(x,t) = \int_0^\infty c(x,t') h(t-t')\,dt', \tag{3}$$

where $h(t)$ is a density function.

Nondimensionalizing Eqs. (1) and (3) by introducing dimensionless variables, $X = x/L_0$, $T = t/\bar{t}$, $C^* = c/C_0$, $q^* = \rho q/\theta_m C_0$, $V = v\bar{t}/L_0$, and $K_D = k_d\rho/\theta_m$, with a linear isotherm: $q_e = k_d c$, Eqs. (1) and (3) can be reduced to the following dimensionless forms,

$$\frac{\partial C^*}{\partial T}(1+K_D) = -V(X)\frac{\partial C^*}{\partial X} - \frac{\partial q^*}{\partial T} \tag{4}$$

and

$$q^*(X,T) = \int_0^\infty C^*(X,T') h(T-T')\,dT', \tag{5}$$

where the reference parameters L_0, $\bar{t}$, and C_0 can be chosen as the length of animal housing, nominal mean residence time ($\bar{t} = V_T/Q$, where V_T (m^3) is the total volume in the system and Q ($m^3\,s^{-1}$) is the volumetric airflow rate), and input concentration, respectively.

Under zero initial conditions of C^* and q^*, and a constant input of unit mass at $X = 0$: $C^*(T, X = 0) = U(T)$, where $U(T)$ is an unit step function defined from the positive direction; Eqs. (4) and (5) can be solved in the Laplace domain,

$$\widehat{C}^*(s) = s^{-1}\exp[-s\tau(1+K_D+\hat{h}(s))] \tag{6}$$

and

$$\hat{h}(s) = \frac{\hat{q}^*(s)}{\widehat{C}^*(s)}, \tag{7}$$

where s is the Laplace variable. In Eq. (6) τ is the residence time of VOC-odor that was released at the inlet $X = 0$ and reached the outlet $X = 1$ with air velocity V under no influence of any rate-limiting processes, and has the form,

$$\tau = \int_0^1 \frac{\mathrm{d}X}{V(X)}. \tag{8}$$

The air velocity V may be envisioned in the microscopic point of view, as a mean projection of the three-dimensionally oriented velocity along the gas-phase trajectory onto the X-coordinate. In Eq. (7), $\hat{h}(s)$ is called the transfer function for the rate-limiting processes.

The dimensionless form of the first-order mass transfer approximation in Eq. (2) can be written as,

$$\frac{\partial q^*}{\partial T} = K(K_{\mathrm{D}} C^* - q^*), \tag{9}$$

where K is the dimensionless rate coefficient, $K = k\bar{t}$. Taking the Laplace transform of Eq. (9) gives

$$\hat{h}(s) = \frac{\hat{q}^*(s)}{\hat{C}^*(s)} = \frac{KK_{\mathrm{D}}}{s + K}. \tag{10}$$

2.2. Statistical ensemble modeling

We are considering now the time history of velocity measured in a ventilated airspace to be representative of a broader set of data. The set of all velocity time histories that would be obtained under sensibly identical conditions involving air exchange rate, air speed and shear, and surface characteristics, for instance, forms an *ensemble* of records, and is viewed as generated by a stochastic process. This ensemble is generally an infinite set of functions. Therefore, we are interested in knowing the probability laws for mixing/adsorption heterogeneity as a physical phenomenon, not just a frequency functions counted from a finite set of finite records.

Liao and Liang [14] developed a model called multiple airflow regions gamma model (MARGM) that is based on a continuous distribution of residence time for predicting the mixing behavior in a ventilated airspace. The MARGM takes the form of a two-parameter gamma distribution and accounts for different mixing patterns such as incomplete, complete–incomplete, incomplete–complete-piston flow, and various combinations of the above types. The applicability of MARGM was tested by several case studies. Simulation results showed that heterogeneous mixing models gave a better fit than a homogeneous one, suggesting that the candidate pdf for the residence time distribution (RTD) τ, $p_\tau(\tau)$ is a two-parameter gamma distribution.

The gamma distribution is a distribution of the Pearson's Type III in statistics. The unique feature of the gamma distribution is that one end of the distribution is bound to a fixed value, whereas the other end is distributed over a large scale of variate. The overall shape of the gamma distribution is not balanced as a normal distribution. The other reason to utilize the gamma distribution is that this approach may reduce the mathematical terms in the analytical solution. The gamma pdf of τ is given by

$$p_\tau(\tau;X=1)\equiv\gamma(\tau;\alpha_\tau,\beta_\tau)=\frac{\beta_\tau^{-\alpha_\tau}\tau^{\alpha_\tau-1}}{\Gamma(\alpha_\tau)}\exp\left(-\frac{\tau}{\beta_\tau}\right), \tag{11}$$

where α_τ (the shape parameter) and β_τ (the scale parameter) are positive parameters, $\Gamma(\alpha_\tau)$ is the gamma function as $\Gamma(\alpha_\tau)=\int_0^\infty \xi^{\alpha_\tau-1}\exp(-\xi)\,\mathrm{d}\xi$, where ξ is a dummy variable of integration, and $p_\tau(\tau;X=1)\,\mathrm{d}\tau$ is the probability for a VOC-odor to have residence time between τ and $\mathrm{d}\tau$ before exiting the system at $X=1$. It should be noted that the mean residence time in dimensionless form is always unity. With the gamma model, the mean and standard deviation of the distribution are $\bar{\tau}=\alpha_\tau\beta_\tau$ and $\mathrm{sd}_\tau=\alpha_\tau^{1/2}\beta_\tau$, respectively.

The shape and scale parameters α_τ and β_τ in the MARGM can be determined by the following relations [14],

$$\alpha_\tau=\begin{cases}\dfrac{V_\mathrm{T}}{V_\mathrm{p}+V_\mathrm{c}+\mu V_i}=\dfrac{1}{\frac{1}{\theta}+\mu\left(1-\frac{1}{\theta}\right)}, & \mu\geqslant 0.5,\\[2ex] \dfrac{V_\mathrm{T}}{V_\mathrm{p}+V_\mathrm{c}+(1-\mu)V_i}=\dfrac{1}{\frac{1}{\theta}+(1-\mu)\left(1-\frac{1}{\theta}\right)}, & \mu\leqslant 0.5,\end{cases} \tag{12}$$

$$\beta_\tau=\frac{1}{\alpha_\tau\left(\frac{V_\mathrm{T}}{V_\mathrm{c}+\mu V_i}\right)}=\frac{1}{\alpha_\tau}\left(\frac{1}{\eta\theta}+\mu-\frac{\mu}{\theta}\right), \tag{13}$$

in which

$$\theta=\frac{V_\mathrm{T}}{V_\mathrm{c}+V_\mathrm{p}} \tag{14}$$

and

$$\eta=\frac{V_\mathrm{T}}{\theta V_\mathrm{c}}, \tag{15}$$

where V_c, V_p and V_i represent the air volumes occupied by complete mixing, piston flow and incomplete mixing, respectively; $V_\mathrm{T}=V_\mathrm{c}+V_\mathrm{p}+V_\mathrm{i}$ is the total volume in the system; μ is the mixing efficiency; θ and η may be referred to as the mixing volume factors I and II, respectively. The mixing efficiency μ is defined to describe the extent of heterogeneous mixing resulting from factors other than molecular diffusion: $\mu=1$ for complete mixing, $\mu=0$ for piston flow, and heterogeneous mixing is characterized by $0<\mu<1$.

In the proposed first-order approximation, some variations in VOC-odor components and within the ambient aerosol size fraction distribution that may cause considerable fluctuations of the local rate process as the VOC-odor diffusion through or adsorbs onto the aerosol surface, are lumped into the two parameters: the equilibrium partition coefficient (K_D) and the adsorption rate constant (K). It is reasonable to treat both K_D and K as randomly distributed variables.

Based on the concept of LFERs [10,15], the logarithms of equilibrium constants associated with changes in reactant structure in parallel reactions should be linearly related to each other and are often negatively correlated. In this study, we employ the LFERs concept to approximate the relationship between the two log-transformed parameters, $\log K_D$ and $\log K$, (i.e., linear $\log K_D \sim \log K$) and thus has the form as,

$$K_D = aK^{-b}, \tag{16}$$

where a and b are two positive constants. As b takes zero or nonzero values, two extreme cases of correlation are represented by Eq. (16), i.e., if $b = 0$, a completely independent relationship exists between K_D and K; whereas any nonzero value of b gives a perfect correlation between K_D and K. Therefore, a perfect correlation would simplify the bivariate pdf ($p_k(K_D; K)$) to being univariate. The resulting univariate pdf can be represented either by the pdf of $K_D(p_d(K_D))$ or by the pdf of $K(p_k(K))$. In this paper, we assume K_D is constant at all adsorption surfaces, thus, a pdf of $K(p_k(K))$ is used to characterize the variations.

Liao et al. [16] recently developed a mathematical model to predict the adsorption rate constant of VOC-odor on the ambient airborne dust based on a gamma distribution of adsorption rates and with the consideration of a distributed Fick's diffusion model as experimental test data. Results showed that the model had successfully fit the test data using a gamma distribution of rate coefficients. The use of a gamma distribution of rate constants is to assume a continuum of "physical lumps" in an ambient aerosol profile with each "lump" being characterized by its own adsorption rate constant.

The gamma pdf of K is given by

$$p_k(K) \equiv \gamma(K; \alpha_k, \beta_k) = \frac{\beta_k^{-\alpha_k} K^{\alpha_k - 1}}{\Gamma(\alpha_k)} \exp\left(-\frac{K}{\beta_k} \right). \tag{17}$$

where α_k is the shape parameter, β_k is the scale parameter, and $\Gamma(\alpha_k)$ is the gamma function. The mean and standard deviation of the distribution are $\overline{K} = \alpha_k \beta_k$ and $\mathrm{sd}_k = \alpha_k^{1/2} \beta_k$, respectively.

Other pdfs may be also available. For example, local VOC-odor diffusion and adsorption rate coefficients have been related to ambient aerosol particle size that is typically considered to be a log–normal distribution [4,5], suggesting

that the log–normal distribution would also be a potential candidate to describe the mass transfer rate distribution. The primary interest of this research, however, is not on the attributions of different pdfs.

By knowing the pdfs of RTD and rate coefficient as shown in Eqs. (11) and (17), the expected output concentration and mean transfer function for the first-order mass transfer can be calculated through Eqs. (6) and (10), respectively, by taking a mathematical expectation operator $E[\cdot]$ in the Laplace domain as,

$$\widehat{C}(X=1,s) = E[\widehat{C}^*(s)] = \int_0^\infty \widehat{C}^*(s) p_\tau(\tau, X=1)\,\mathrm{d}\tau \tag{18}$$

and

$$\widehat{H}(s) = E[\hat{h}(s)] = \int_0^\infty \frac{aK^d}{s+K} p_k(K)\,\mathrm{d}K. \tag{19}$$

where $d = 1 - b$. By substituting Eqs. (11), (16) and (17), into Eqs. (18) and (19), respectively, the final expression is,

$$\widehat{C}(X=1,s) = \int_0^\infty \int_0^\infty s^{-1} \exp[-s\tau(1 + aK^{-b} + \hat{H}(s))]\gamma(K;\alpha_k,\beta_k)\gamma(\tau;\alpha_\tau,\beta_\tau)\,\mathrm{d}K\,\mathrm{d}\tau, \tag{20}$$

where $\widehat{H}(s)$ has the following forms as

$$\widehat{H}(s) = \int_0^\infty \frac{aK^d}{s+K}\gamma(K;\alpha_k,\beta_k)\,\mathrm{d}K, \tag{21}$$

Eq. (21) reveals that ensemble transfer function includes four parameters: two common constants, a and d ($d = 1 - b$); two specific, α_k and β_k. The four parameters, however, may be reduced to three after subjecting the constraint of the sample-averaged K_D as,

$$E[K_\mathrm{D}] = \overline{K}_\mathrm{D} = aE[K^{-b}], \tag{22}$$

where $E[K^{-b}]$ is the bth moment in the statistical sense,

$$E[K^{-b}] = \beta_k^b \frac{\Gamma(\alpha_k - b)}{\Gamma(\alpha_k)}. \tag{23}$$

Substituting Eq. (23) into Eq. (22) results in four parameters that are all constrained to the known value of $E[K_\mathrm{D}]$. This means that whenever three of them are chosen, the fourth is automatically determined by Eq. (22).

The inverse Laplace transform of $\widehat{C}(X=1,s)$ in Eq. (20) provides an expected concentration output across the exit plane at $X = 1$ under the corresponding unit step input boundary conditions in a ventilation system. In the

case of a Dirac (impulse) input boundary condition were also discussed later in that $\widehat{C}^*(s)$ in Eq. (6) becomes

$$\widehat{C}^*(s) = \exp[-s\tau(1 + K_{\mathrm{D}} + \hat{h}(s))]. \tag{24}$$

Fig. 2 illustrates a conceptual algorithm showing the system process, system transfer function, governing equations and computational procedures.

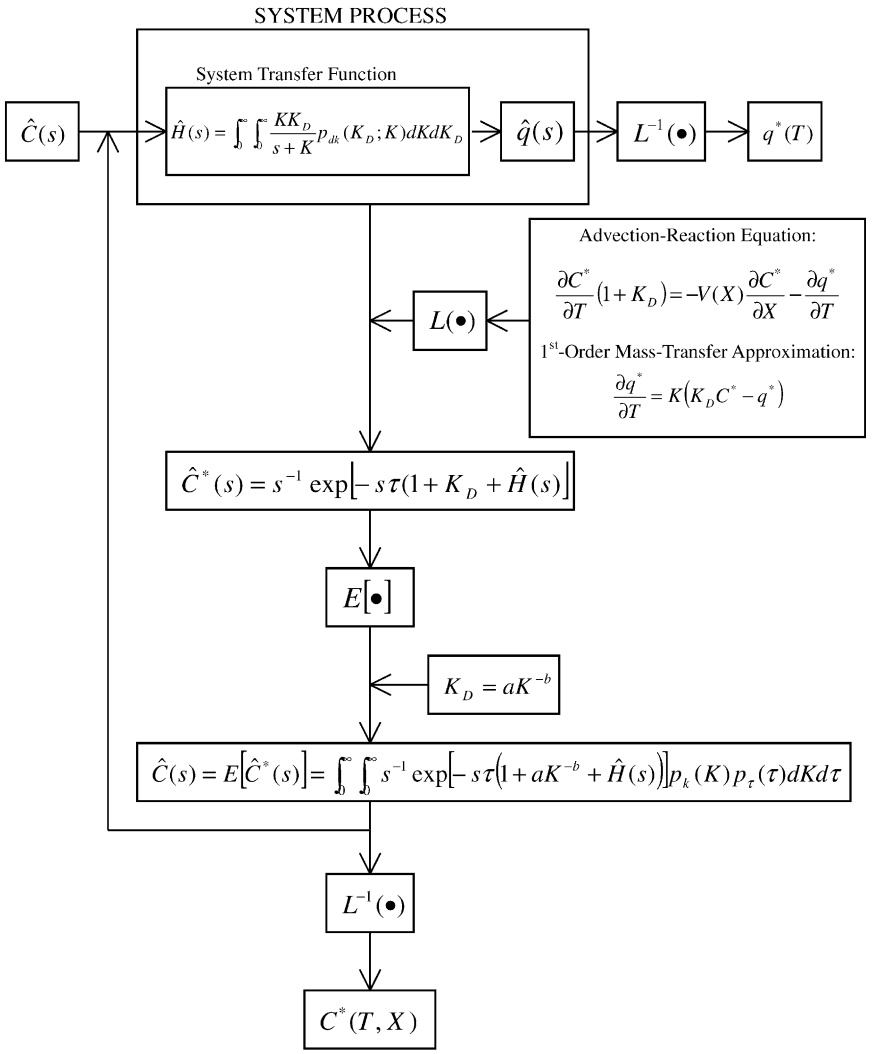

Fig. 2. Schematic illustration of a conceptual algorithm showing the system transport process, system transfer function, governing equations, and computational procedures in the case of a boundary unit step response function.

Analytical inversion of Eq. (20) may be possible yet would probably lead to complex integrals. Therefore, numerical inversion to obtain the solution is adopted. Numerous algorithms that have been successfully applied to numerically invert the Laplace transformed analytical solution include the Stehfest algorithm [17], the Talbot algorithm [18], the Crump algorithm [19] and the de Hoog et al. algorithm [20]. In the present research, we selected the de Hoog et al. algorithm, a modified fast Fourier transform algorithm, to perform the inversion of Eq. (20) because it provides a good accuracy for a wide variety of functions and it also performs reasonably well in the neighborhood of a discontinuity (i.e., the shape front). The Laplace transform parameter has to be declared as a complex variable in computation when the de Hoog et al. algorithm is used. A FORTRAN subroutine DINLAP/LINAP [21] based on the de Hoog et al. algorithm is employed to perform the Laplace transform. (The program is available upon request from the authors.)

3. Model analysis

The effects of mean adsorption rate coefficient ($\overline{K}$), mean residence time of VOC-odor ($\bar{\tau}$), mean partitioning coefficient ($\overline{K}_{\mathrm{D}}$), coefficient of variation (CV) for K and τ (CV_k and CV_τ) on VOC-odor transport were performed systematically as seven cases based on the input parameters given in Table 1. Three different mixing patterns, incomplete mixing, complete–incomplete mixing, and complete–incomplete-piston flow, are applied in this study.

Simulation results in the cases of impulse and unit step inputs boundary conditions are presented in Figs. 3–6. Table 2 gives the calculated peak concentrations and the time to peak concentrations, whereas Table 3 listed the calculated equilibrium concentrations and the times to 99% equilibrium concentration. Generally, the equilibrium concentrations are higher than the peak concentrations at the same simulation conditions (Tables 2 and 3).

Comparison between model simulated output dynamics from the mixing/adsorption heterogeneity under different $\overline{K}$ values at different $\bar{\tau}$ of 1 and 4 is illustrated in Fig. 3 (for cases 1 and 2). Fig. 3 shows that the peak and the equilibrium concentrations of the output curves decreased as the $\overline{K}$ values increased from 4 to 100, indicating high dependence upon the relative adsorption rate coefficient during the transport process.

When the $\overline{K}$ value is low, sorption is generally slower than transport and nonequilibrium conditions are present. This implies that most VOC-odor bypass a continuum of adsorption surfaces of airborne dust, resulting in a sharp peak and a very small amount of sorbed VOC-odor to produce a flattened curve tail (Fig. 3A and B). In the high $\overline{K}$ value case, nonequilibrium conditions are less severe, and most VOC-odors have sufficient time to diffuse to or react

Table 1
Input parameter used for simulation of VOC-odor transport under mixing/adsorption heterogeneity

Mixing pattern	Cases	$\overline{K}$	α_k	β_k	CV_k	α_τ	β_τ	CV_τ	a	b	$\overline{K}_D$	μ[a]
Incomplete[b]	1a	4	2	2	0.707	1	1	1	2	1	4	0.502
	1b	10	5	2	0.707	1	1	1	2	1	1	0.502
	1c	40	20	2	0.707	1	1	1	2	1	0.211	0.502
	1d	100	50	2	0.707	1	1	1	2	1	0.082	0.502
	2a	4	2	2	0.707	4	1	1	2	1	4	0.502
	2b	10	5	2	0.707	4	1	1	2	1	1	0.502
	2c	40	20	2	0.707	4	1	1	2	1	0.211	0.502
	2d	100	50	2	0.707	4	1	1	2	1	0.082	0.502
	3a	4	2	2	0.707	2	1	1	2	1	4	0.502
	3b	4	20	0.2	2.236	2	1	1	2	1	0.021	0.502
	4a	0.4	2	0.2	2.236	2	2	0.707	2	1	0.4	0.502
	4b	1	2	0.5	1.414	2	2	0.707	2	1	1	0.502
	4c	10	2	5	0.447	2	2	0.707	2	1	10	0.502
	4d	40	2	20	0.224	2	2	0.707	2	1	40	0.502
	4e	100	2	50	0.141	2	2	0.707	2	1	100	0.502
Complete–incomplete[b]	5a	10	2	5	0.447	2	0.2	2.236	2	1	10	0.671
	5b	10	2	5	0.447	0.2	2	0.707	2	1	10	0.671
	6a	10	2	5	0.447	2	2	0.707	2	1	10	0.671
	6b	10	2	5	0.447	5	0.8	1.124	2	1	10	0.671
Complete–incomplete-piston[b]	7a	4	2	2	0.707	2	2	0.707	1	0	1	0.312
	7b	4	2	2	0.707	2	2	0.707	10	0	10	0.312
	7c	4	2	2	0.707	2	2	0.707	2	0.1	1.07	0.312
	7d	4	2	2	0.707	2	2	0.707	2	1	4	0.312

[a] Values are determined based on Eqs. (12)–(15).
[b] Mixing pattern is determined based on the relations of $V_T = V_c + V_p + V_i$ and Eq. (11).

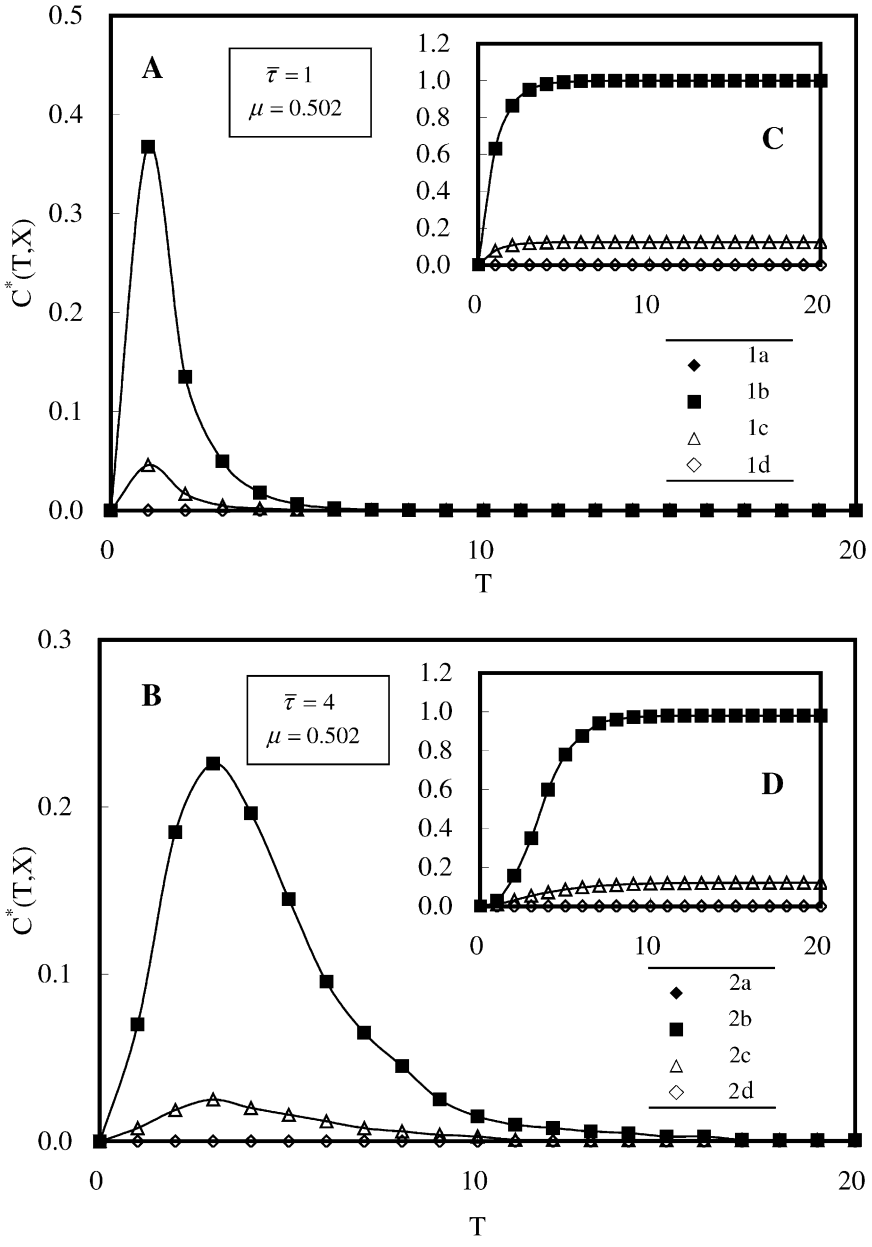

Fig. 3. Effect of mean adsorption rate coefficient ($\overline{K}$) on output VOC-odor concentration in an incomplete mixing regime ($\mu = 0.502$) for impulse (A and B) and unit step (C and D) response functions based on cases 1 and 2.

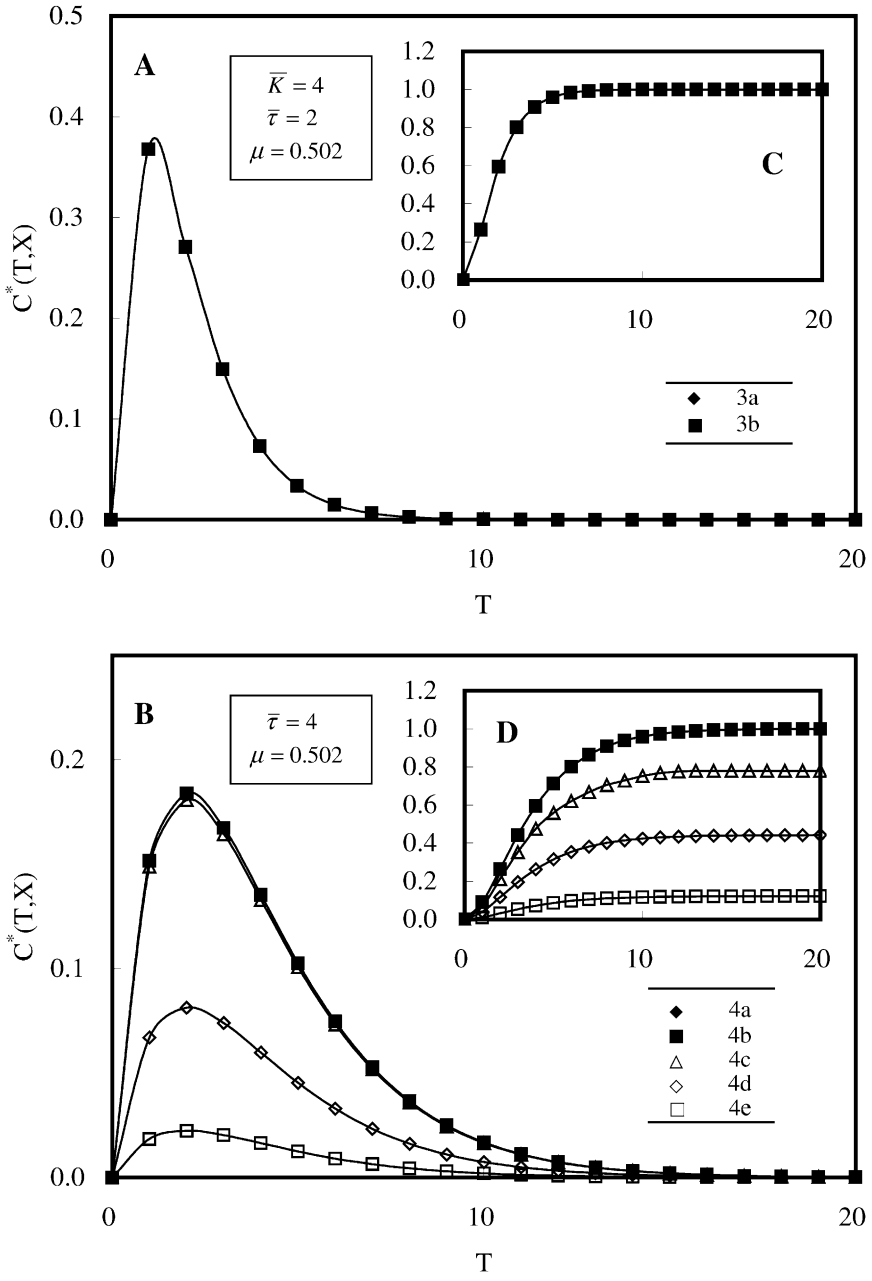

Fig. 4. Effect of CV of $K(\mathrm{CV}_k)$ on output VOC-odor concentration in an incomplete mixing regime ($\mu = 0.502$) for impulse (A and B) and unit step (C and D) response functions based on cases 3 and 4.

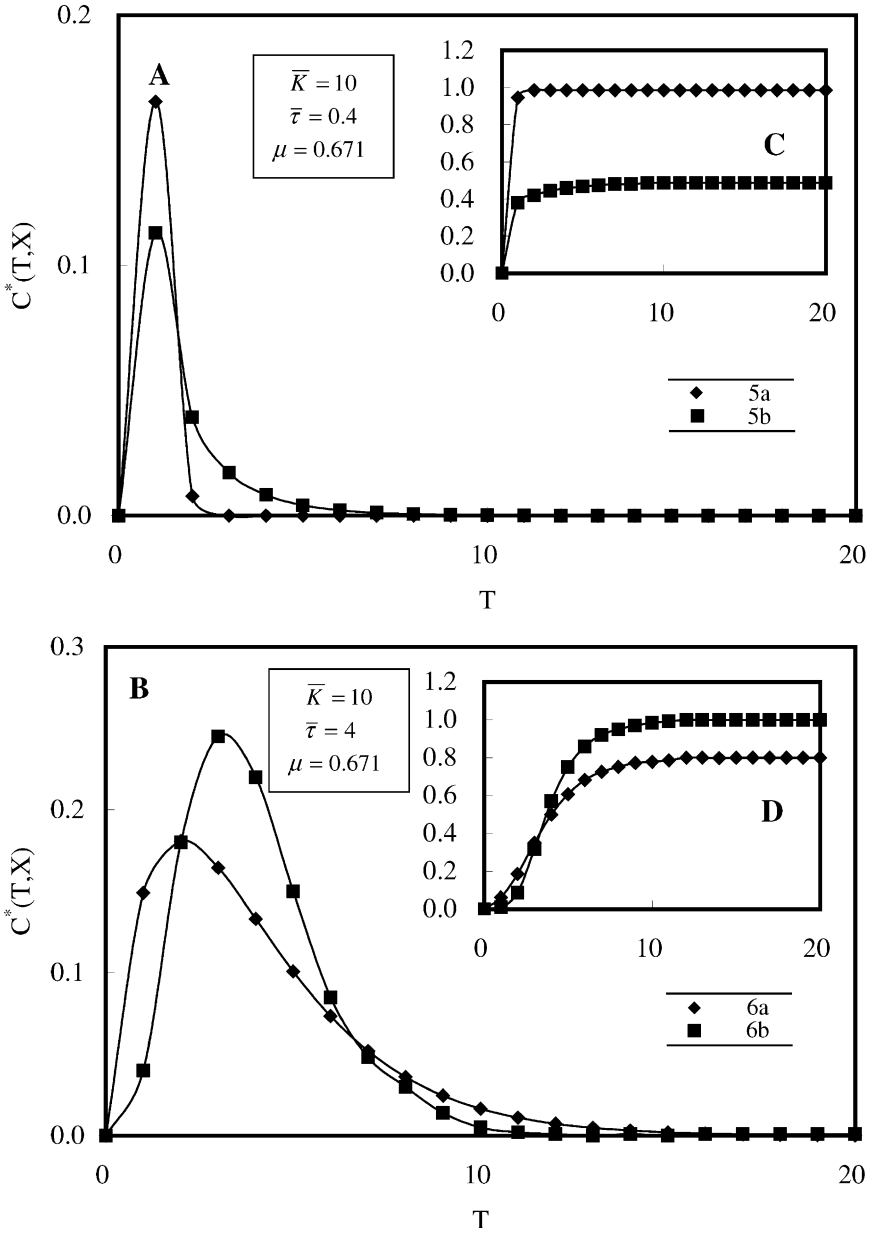

Fig. 5. Effect of CV of $\tau(CV_\tau)$ and mean residence time $(\overline{\tau})$ on output VOC-odor concentration in a complete–incomplete mixing regime ($\mu = 0.671$) for impulse (A and B) and unit step (C and D) response functions based on cases 5 and 6.

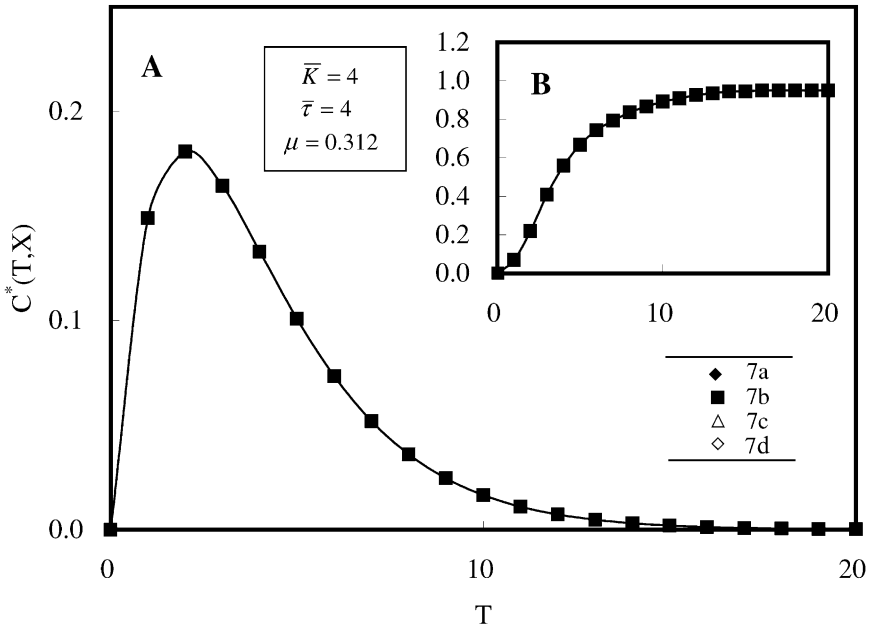

Fig. 6. Effect of mean linear partitioning coefficient ($\overline{K}_D$) on output VOC-odor concentration in a complete–incomplete-piston flow mixing regime ($\mu = 0.312$) for impulse (A) and unit step (B) response functions based on case 7.

with the continuum of adsorption surfaces of ambient aerosol, giving a wider peak.

When the model less affected by $\overline{K}$, further indicating the complimentary effect of assuming a range of sorption surfaces. As seen from the current simulations where the same $CV_k = 0.707$ were both used for K in cases 1 and 2, substantial deviation between output curves still exists, indicating sorption surface heterogeneity. The high dependence on $\overline{K}$ may also imply that this model can be highly air velocity-dependent.

The effects of different CV_k and K at $\bar{\tau}$ of 1 and 4 are shown in Fig. 4 (for cases 3 and 4) in that Fig. 4A and C has the same $\overline{K}$ but different CV_k, whereas the different $\overline{K}$ and CV_k for Fig. 4B and D. Theoretically, when the value of the CV_k tends to zero, representing homogeneous sorption behavior. Fig. 4B shows that an apparently higher variability of sorption rate would spread the VOC-odor peak more significantly, peak spreading is limited in the model since the increase of the sorption rate variability means that the rate deviation increases between the distinct surfaces. That is to say, the higher $\overline{K}$ values at lower CV_k results in a distributed instead of a more sharpened peak.

Table 2 indicates that in the cases 4, the predicted peak concentration varied by up to one order of magnitude as the order of magnitude of $\overline{K}$ values

Table 2
Calculated peak concentrations and the time to peak concentrations in the case of impulse response function

Cases	Peak concentration (—)	Time to peak concentration (—)
1a	0.368	1
1b	0.367	1
1c	0.046	1
1d	3.81×10^{-13}	1
2a	0.224	3
2b	0.223	3
2c	0.028	3
2d	1.83×10^{-13}	3
3a	0.368	1
3b	0.367	1
4a	0.185	2
4b	0.184	2
4c	0.181	2
4d	0.081	2
4e	0.022	2
5a	0.166	1
5b	0.113	1
6a	0.181	2
6b	0.238	3
7a	0.184	2
7b	0.184	2
7c	0.184	2
7d	0.184	2

increasing from <10 to 10^2, but not for the unit step response function presented in Table 3.

Fig. 5 (for cases 5 and 7) compares the influence of different $\bar{\tau}$ and CV_τ values on the simulation results. When the $\bar{\tau}$ values is high, the peak and the equilibrium concentrations are generally higher and the times to the peak and the equilibrium concentrations are longer as well (Tables 2 and 3). At large residence time ($\bar{\tau}$) means at low airflow rate as well, the VOC-odor remains longer in the ventilated airspace, indicating that there is more time for diffusion into airborne dust. This causes the differences between the output curves at different $\bar{\tau}$ values. The shape of the output curve is then determined by the ratio of airflow rate and adsorption rate. Fig. 5C shows that higher CV_τ values would spread the VOC-odor peak more significantly, indicating heterogeneous mixing behavior. In the present study, the form of dispersion is not included in the model. Dispersion, however, mainly affects the initial part of the output curve and becomes less significant when diffusion into airborne dust becomes more important.

Table 3
Calculated equilibrium concentrations and the time to 99% equilibrium concentrations in the case of step response function

Cases	Equilibrium concentration (—)	Time to equilibrium concentration (—)
1a	0.992	5
1b	0.991	5
1c	0.124	5
1d	1.13×10^{-24}	5
2a	0.993	11
2b	0.992	11
2c	0.124	11
2d	8.45×10^{-13}	11
3a	0.993	8
3b	0.993	8
4a	0.994	11
4b	0.989	11
4c	0.797	11
4d	0.438	11
4e	0.121	11
5a	0.979	2
5b	0.483	2
6a	0.797	11
6b	0.983	11
7a	0.902	11
7b	0.902	11
7c	0.902	11
7d	0.902	11

The influence of different $\overline{K}_D$ values on the simulation results is illustrated in Fig. 6 (for case 7). As was shown in Fig. 6, the simulation results indicate that $\overline{K}_D$ values have less influence on output profiles. An increase in $\overline{K}_D$ increases the peak as well as the concentration level in the output curves. Therefore, when a pdf of K is incorporated into the model, a change in $\overline{K}_D$ would not significantly change the model predictions. This indicates that the present model, with no correlation between K_D and K, may approximate the cases where K_D and K are not strictly correlated (as in Eq. (16)).

Results of this simulation study show that when mixing/adsorption heterogeneity exists, simple assumptions are questionable to sufficiently represent a more generally distributed adsorption process. The attempt to lump the effect of nonequilibrium processes into an effective dispersion coefficient or to find a simple equivalent representation for a more complex mechanistic model may be effective for homogeneous systems having a uniform equilibration rate or adsorption properties and for processes over a relatively short time scale. This observation will be further verified with experimental data in the subsequent work on VOC-odor transport.

4. Conclusions

For a heterogeneous mixing/adsorption system in a ventilated airspace, which is characterized by a wide particle size distribution, particle surface, heterogeneous physicochemical–biological composition on particle surface, and various mixing patterns, the transport of VOC-odor is inherently complex.

Any mathematical model, assumption may bias results. The present model assumes isotherm linearity. The concept of sorption equilibrium which proposes that, given a sufficient time, a predictable ratio of gaseous-phase to adsorbed-phase VOC-odor will occur for any airborne dust/VOC-odor compositions. There are many complicating issues in developing this correlation, such as the difficulty in determining an appropriate partitioning coefficient and correlation to airflow velocity or adsorption rate coefficient.

It is likely that the heterogeneity of the physicochemical/biological characteristics of airborne dust/VOC-odor compositions and the resulting variability of adsorption rates was large, requiring the diversity of rate controls inherent in the sophisticated kinetic model for successful prediction of the adsorption and transport of VOC-odor in a ventilated airspace within a dusty medium.

Additional experiments are needed to establish the generality of the model. The implication of the present predictive model is that there are heterogeneous rate controls on the adsorption of the VOC-odor on the aerosol surface, and there are heterogeneous air mixing that affect the residence time of VOC-odor and consequently affect the effectiveness performance of a ventilation system. Inclusion of an instantaneous equilibrium "lump" and a nonequilibrium "lump" with a distribution of adsorption rate coefficients was needed to successfully predict transport behavior. Thus, this complex description of adsorption kinetics and incomplete mixing of air was required.

References

[1] R.H. Zhang, P.N. Dugba, D.S. Bundy, Laboratory study of surface aeration of anaerobic lagoons for odor control of swine manure, Trans. ASAE 40 (1) (1997) 185–190.
[2] J. Zhu, D.S. Bundy, X. Li, N. Rashid, Controlling odor and volatile substances in liquid hog manure by amendment, J. Environ. Qual. 26 (3) (1997) 740–743.
[3] C.M. Liao, H.M. Liang, S. Singh, Exposure assessment model for odor causing VOCs volatilization from stored pig slurry, J. Environ. Sci. Health B 33 (4) (1998) 457–486.
[4] C.M. Liao, S. Singh, Modeling dust-borne odor dynamics in swine housing based on age and size distributions of airborne dust, Appl. Math. Modell. 22 (9) (1998) 671–685.
[5] C.M. Liao, J.S. Chen, J.W. Chen, Dynamic model for predicting dust-borne odour concentrations in ventilated animal housing, Appl. Math. Modell. 24 (2) (2000) 131–145.
[6] J. Zhu, A review of microbiology in swine manure odor control, Agric. Ecosyst. Environ. 78 (2000) 93–106.
[7] E.M. Barber, J.R. Ogilvie, Incomplete mixing in ventilated airspaces. Part I. Theoretical considerations, Can. Agric. Eng. 24 (1) (1982) 25–29.

[8] Y.C. Chen, E.M. Barber, Y. Zhang, R.W. Besant, S. Sokhansanj, Methods to measure dust production and deposition rates in buildings, J. Agric. Eng. Res. 72 (1992) 329–340.
[9] G.P. Box, G.M. Jenkins, Time Series Analysis Forecasting and Control, Prentice-Hall, Englewood Cliffs, NJ, 1976.
[10] W.J. Weber, F.A. DiGiano, Process Dynamics in Environmental Systems, Wiley, New York, 1995.
[11] C.M. Liao, J.J.R. Feddes, A lumped-parameter model for predicting airborne dust concentration in a ventilated airspace, Trans. ASAE 35 (6) (1992) 1973–1978.
[12] O. Liu, S.J. Hoff, G.M. Maxwell, D.S. Bundy, Comparison of three κ–ϵ turbulence models for predicting ventilation air jets, Trans. ASAE 39 (2) (1996) 689–698.
[13] S.J. Hoff, D.S. Bundy, Comparison of contaminant dispersion modeling approaches for swine housing, Trans. ASAE 39 (3) (1996) 1151–1157.
[14] C.M. Liao, H.M. Liang, Characterization of mixing patterns in a ventilated airspace with a multiple airflow regions gamma model, J. Environ. Sci. Health A 36 (3) (2000) 333–353.
[15] J.W. Moore, R.G. Pearson, Kinetics and Mechanism, third ed., Wiley, New York, 1981.
[16] C.M. Liao, Y.L. Yeh, J.S. Chen, J.W. Chen, Modeling lumped-parameter sorption kinetics and diffusion dynamics of odor causing VOCs to dust particles, Appl. Math. Modell. 25 (2000) 593–611.
[17] H. Stehfest, Numerical inversion of Laplace transforms, Commun. ACM 13 (1970) 47–49.
[18] A. Talbot, The accurate numerical inversion of Laplace transforms, J. Inst. Math. Appl. 23 (1979) 97–120.
[19] K.S. Crump, Numerical inversion of Laplace transforms using a Fourier series approximation, J. Assoc. Comput. Mech. 23 (1976) 89–96.
[20] F.R. de Hoog, J.H. Knight, A.N. Stocks, An improved method for numerical inversion of Laplace transforms, SIAM J. Sci. Stat. Comput. 3 (3) (1982) 357–366.
[21] IMSL MATH/LIBRARY, FORTRAN Subroutine for Mathematical Applications, vols. 1 and 2, Visual Numerics, Houston, TX, 1994.